Model-Based Predictive Control Applied to the Doubly-Fed Induction Generator Direct Power Control

Alfeu J. Sguarezi Filho, *Member, IEEE*, and Ernesto Ruppert Filho

***Abstract*—This paper proposes a model-based predictive controller for doubly-fed induction generator direct power control. The control law is derived by optimization of an objective function that considers the control effort and the difference between the predicted outputs (active and reactive power) and the specific references, with predicted outputs calculated using a linearized state-space model. In this case, the controller uses active and reactive power loop directly for the generator power control. Because the generator leakage inductance and resistance information were required for this control method, the influence of the estimation errors for these parameters was also investigated. Simulation results are carried out to validate the proposed controller.**

***Index Terms*—Direct power control, doubly-fed induction generator (DFIG), model-based predictive control, wind energy.**

I. Introduction

THE wind energy systems using a doubly-fed induction generator (DFIG) have some advantages due to variable speed operation and four quadrant active and reactive power capabilities compared with fixed speed induction generators and synchronous generators. The stator of DFIG is connected directly to the grid, and the rotor links the grid by a bidirectional converter; its rated power is much more minor than the DFIG rated power although the power converters used in squirrel cage induction or synchronous generators has to support the rated power of the machine. The rotor converter objective aims to the DFIG active and reactive power control between the stator and ac supply [1], [2]. The configuration of DFIG connected directly on the grid is shown in Fig. 1.

DFIG wind turbine systems control is traditionally based on either stator-flux-oriented [3] or stator-voltage-oriented [4] vector control. The scheme decouples the rotor current into active and reactive power components. The active and reactive power control is achieved with a rotor current controller. Some investigations use PI controllers by using stator-flux-oriented controllers that generate reference currents from active and reactive power errors to the inverter or cascade PI controllers that generate a rotor voltage which has been presented by [5]. The problem in the use of a PI controller is the tuning of the gains and the cross-coupling on DFIG terms in the whole operating range. Interesting methods that try to solve these problems have been presented by [6]–[8].

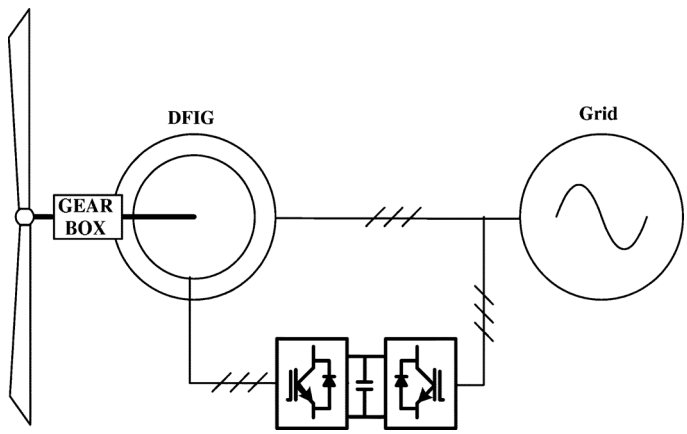

Fig. 1. Configuration of DFIG connected directly on grid.

Some investigations using a predictive functional controller [9] and internal mode controller [10], [11] have satisfactory power response when compared with the power response of PI, but it is hard to implement one due to the predictive functional controller and internal mode controller formulation. Another possibility of doubly-fed power control can be made by using fuzzy logic [12], [13]. These strategies have satisfactory power response although it involves relatively complex transformation of voltages, currents, and control outputs among the stationary, the rotor, and the synchronous reference frames.

An alternative for DFIG power control based in direct torque control principles [14], [15] is the direct power control (DPC) that initially was applied to the three-phase PWM rectifiers, which has been presented in [16]. The converter switching states were selected from an optimal switching table based on the instantaneous errors between the reference and estimated values of active and reactive power and the angular position of the estimated converter terminal voltage vector.

The DPC applied to the DIFG power control has been presented in [17]–[19]. This scheme calculates the required rotor controlling voltage directly based on the estimated stator flux, active and reactive power, and their errors. The implementation of DPC using hysteresis controllers was presented in [17] and the principles method are described in [18], [19]. Moreover, the

Manuscript received December 27, 2010; revised November 01, 2011; accepted December 26, 2011. Date of publication April 18, 2012; date of current version June 15, 2012. This work was supported in part by FAPESP and CNPq.

A. J. Sguarezi Filho is with the Center of Engineering, Modeling, and Applied Social Sciences, Universidade Federal do ABC—UFABC, Santo André 09.210-170, Brazil (e-mail: alfeu.sguarezi@ufabc.edu.br).

E. R. Filho is with the School of Electrical and Computer Engineering, Campinas University—UNICAMP, Campinas 13083-970, Brazil (e-mail: ruppert@fee.unicamp.br).

Color versions of one or more of the figures in this paper are available online at http://ieeexplore.ieee.org.

Digital Object Identifier 10.1109/TSTE.2012.2186834

conventional DPC complicates the ac filter design because of its variable switching frequency. To eliminate the torque ripple and use constant switching frequency, an antijamming controller was proposed in [20].

The concept of DPC was applied to DFIG under unbalanced grid voltage conditions by [21] and [22]. In [21], the active and reactive powers were made to track references using hysteresis controllers. In [22], a notch filter was applied in DPC strategy which allows the power control. These strategies have satisfactory active and reactive power response under unbalanced grid voltage.

The predictive control is an alternative control technique that was applied in machine drives and inverters [23], [24]. Some investigations such as long-range predictive control [25], general predictive control [23], and model predictive control were applied to the induction motor drives. The predictive functional control and model predicitve were applied to the DFIG power control by using rotor currents in [9] and [27], respectively. A predictive DPC for DFIG was presented in [28]. These strategies have a satisfactory power response although the control does not predict the outputs (active and reactive power or rotor current) and it can degradate the power response. A solution that allows us to predict the outputs using a rotor current control of DFIG was presented in [29].

This paper proposes a model-based predictive controller for DFIG DPC. The control law is derived by optimization of an objective function that considers the control effort and the difference between the predicted outputs (active and reactive power) and the specific references, with predicted outputs calculated using a linearized state-space model. Because the generator leakage inductance and resistance information were required for this control method, the influence of the estimation errors for these parameters was also investigated. The contribution is in applying this control technique for controlling directly the active and reactive power of DFIG without using rotor current loop. So, the DFIG was modeled using the active and reactive power as state variables and the rotor voltage vector as input. In this case, the MBPC for DFIG DPC uses only active and reactive power loops and it is an alternative for PI regulators that is also used in rotor current vector control. Simulation results are carried out to validate the proposed controller.

II. Doubly-Fed Induction Machine Model and DPC

The doubly-fed induction machine model in synchronous reference frame is given by [30]

$$\vec{v}_{1dq} = R_1\vec{i}_{1dq} + \frac{d\vec{\lambda}_{1dq}}{dt} + j\omega_1\vec{\lambda}_{1dq} \tag{1}$$

$$\vec{v}_{2dq} = R_2\vec{i}_{2dq} + \frac{d\vec{\lambda}_{2dq}}{dt} + j(\omega_1 - PP\omega_{\rm mec})\vec{\lambda}_{2dq} \tag{2}$$

the relationship between fluxes and currents are

$$\vec{\lambda}_{1dq} = L_1\vec{i}_{1dq} + L_M\vec{i}_{2dq} \tag{3}$$

$$\vec{\lambda}_{2dq} = L_M\vec{i}_{1dq} + L_2\vec{i}_{2dq} \tag{4}$$

and generator active and reactive power are

$$P = \frac{3}{2}(v_{1d}i_{1d} + v_{1q}i_{1q}) \tag{5}$$

$$Q = \frac{3}{2}(v_{1q}i_{1d} - v_{1d}i_{1q}). \tag{6}$$

The subscripts 1 and 2 represent the stator and rotor parameters, respectively, ω_1 is the synchronous speed, $\omega_{\rm mec}$ is the machine speed, R_1 and R_2 are the stator and rotor windings per phase electrical resistance, L_1 and L_2 are the proper inductances of the stator and rotor windings, L_M is mutual inductance, $\vec{v}$ is the voltage vector, $\vec{i}$ is the current vector, $\vec{\lambda}$ is the flux vector, and PP is the machine number of pair of poles.

DPC aims independent stator active P and reactive Q power control by means of a rotor flux regulation. For this purpose, P and Q are represented as functions of each individual rotor flux. Using stator flux oriented control, that decouples the dq axis which means $\lambda_{1d} = \lambda_1 = |\vec{\lambda}_{1dq}|$ and $\lambda_{1q} = 0$, (3) and (4), the relationship between stator currents and rotor fluxes is given by

$$i_{2d} = \frac{L_1}{L_1L_2 - L_M^2}\lambda_{2d} - \frac{L_M}{L_1}\frac{L_1}{L_1L_2 - L_M^2}\lambda_1 \tag{7}$$

$$i_{2q} = \frac{L_M}{L_1L_2 - L_M^2}\lambda_{2q} \tag{8}$$

and the active (5) and reactive (6) power can be computed by using (7) and (8)

$$P = -\frac{3v_1L_M}{2\sigma L_1L_2}\lambda_{2q} \tag{9}$$

$$Q = \frac{3v_1L_M}{2\sigma L_1L_2}\left(-\lambda_{2d} + \frac{L_2}{L_M}\lambda_1\right) \tag{10}$$

where $v_1 = v_{1q} = |\vec{v}_{1dq}|$ and $\sigma = 1 - (L_M^2)/(L_1L_2)$.

Equation (2) indicates that the rotor flux change is directly controlled by the applied rotor voltage when rotor resistance is neglected. Thus, rotor fluxes will reflect on stator active and reactive power as can be seen in (9) and (10). Consequently, this principle can be used on stator active and reactive power control on the rotor side in the DFIG with stator connected to the grid.

A. Rotor Side Equations

Equation (2) indicates that the rotor flux change is directly controlled by the applied rotor voltage and it can be used on DFIG power control. The rotor voltage (2), neglecting the rotor resistance, in synchronous referential frame using the stator flux position and active (9) and reactive (10) power becomes

$$\frac{dQ(t)}{dt} = \frac{v_{2d}(t)}{Am} + \omega_{\rm sl}P(t) \tag{11}$$

and

$$\frac{dP(t)}{dt} = \frac{v_{2q}(t)}{Am} - \omega_{\rm sl}Q(t) - \omega_{\rm sl}\frac{L_2}{L_M\ Am}\lambda_1 \tag{12}$$

where $\omega_{\rm sl} = \omega_1 - PP\omega_{\rm mec}$ and $Am = -(2\sigma L_1L_2)/(3v_1L_M)$.

In space state form, (11) and (12) become

$$\begin{aligned}\dot{\bar{x}} &= A\bar{x} + B\bar{u} + G\bar{\omega}\\ \bar{y} &= C\bar{x}\end{aligned} \tag{13}$$

$$\begin{bmatrix}\dot{Q}\\ \dot{P}\end{bmatrix} = \begin{bmatrix}0 & \omega_{\rm sl}\\ -\omega_{\rm sl} & 0\end{bmatrix}\begin{bmatrix}Q\\ P\end{bmatrix} + \begin{bmatrix}\frac{1}{Am} & 0\\ 0 & \frac{1}{Am}\end{bmatrix}\begin{bmatrix}v_{2d}\\ v_{2q}\end{bmatrix} + \begin{bmatrix}1 & 0\\ 0 & 1\end{bmatrix}\begin{bmatrix}0\\ -\dfrac{\omega_{\rm sl}L_2}{L_M\, Am}\lambda_1\end{bmatrix} \tag{14}$$

where $C = I$ and I is the identity matrix.

Due to the fact that the mechanical time constant is much greater then the electrical time constants. Thus $\omega_{\rm mec} =$ constant is a valid approximation for each sample period [31]–[33]. Hence the slip speed $\omega_{\rm sl} =$ constant, due to the synchronous speed $\omega_1 = 2\pi f$ was fixed by the grid and $f = 60$ Hz.

Equation (14) can be discretized considering T as the sampling period and k as the sampling time by using zero-order-hold (ZOH) [34]–[36] with no delay as

$$\begin{aligned}\bar{x}(k+1) &= A_d\bar{x}(k) + B_d\bar{u}(k) + G_d\bar{\omega}_d(k)\\ \bar{y}(k+1) &= C_d\bar{x}(k+1)\end{aligned} \tag{15}$$

where

$$\begin{aligned}A_d &= e^{AT} \cong I + AT\\ B_d &= \int_0^\tau e^{AT}Bd\tau \cong BT\\ G_d &= \int_0^\tau e^{AT}Gd\tau \cong GT\\ C_d &= C.\end{aligned} \tag{16}$$

Due to the applied rotor, voltage is constant during a power control period for voltage-fed PWM. Thus, (14) discretized using (16) is given by

$$\begin{bmatrix}Q(k+1)\\ P(k+1)\end{bmatrix} = \begin{bmatrix}1 & \omega_{\rm sl}T\\ -\omega_{\rm sl}T & 1\end{bmatrix}\begin{bmatrix}Q(k)\\ P(k)\end{bmatrix} + \begin{bmatrix}\frac{T}{Am} & 0\\ 0 & \frac{T}{Am}\end{bmatrix}\begin{bmatrix}v_{2d}(k)\\ v_{2q}(k)\end{bmatrix} + \begin{bmatrix}1 & 0\\ 0 & 1\end{bmatrix}\begin{bmatrix}0\\ \dfrac{-\omega_{\rm sl}L_2T}{L_MAm}\lambda_1(k)\end{bmatrix}. \tag{17}$$

So, the DFIG was modeled using the active and reactive power as state variables and the rotor voltage vector as input in (17), and this model can be applied to the model-based predictive control for a DPC strategy.

III. Model-Based Predictive Control Applied to the DPC

The model-based predictive control (MBPC) consists of two main elements: the model of the system to be controlled and the optimizer which determines optimal future control actions. The model is used to predict the future behavior of the system with the control law obtained by optimizing a cost function that considers the effort necessary for control and the difference between the output predicted and the actual reference value.

The receding-horizon principle is used so that the first element of the optimal sequence is applied. In any plant, new measurements are made for each succeeding sample, and the procedures are then repeated.

There are various MBPC techniques for output prediction by using the state space model or the transfer function of the system [37], [38], [26], [39], [29]. In this paper, the output prediction is derived from the state space model and it is given by

$$Y = P_{px}\bar{x}(k) + HU + D\bar{\omega}_d(k) \tag{18}$$

where

$$Y = [\,y(k+1) \quad y(k+2) \quad \cdots \quad y(k+n_y)\,]^T \tag{19}$$

$$U = [\,u(k) \quad u(k+1) \quad \cdots \quad u(k+n_y-1)\,]^T \tag{20}$$

$$P_{px} = [\,C_dA_d \quad C_dA_d^2 \quad C_dA_d^3 \quad \cdots \quad C_dA_d^{n_y}\,]^T \tag{21}$$

$$H = \begin{bmatrix} C_dB_d & 0 & 0 & \cdots\\ C_dA_dB_d & C_dB_d & 0 & \cdots\\ C_dA_d^2B_d & C_dA_dB_d & C_dB_d & \cdots\\ \vdots & \vdots & \vdots & \vdots\\ C_dA_d^{n_y-1}B_d & C_dA_d^{n_y-2}B_d & C_dA_d^{n_y-3}B_d & \cdots \end{bmatrix} \tag{22}$$

$$D = \begin{bmatrix} C_d & 0 & 0 & \cdots & 0\\ C_dA_d & C_d & 0 & \cdots & 0\\ C_dA_d^2 & C_dA_d & C_d & \cdots & 0\\ \vdots & \vdots & \vdots & \vdots & \\ C_dA_d^{n_y-1} & C_dA_d^{n_y-2} & C_dA_d^{n_y-3} & \cdots & C_d \end{bmatrix} \tag{23}$$

where n_y is the prediction horizon output.

As the DFIG was modeled using the active and reactive power as state variables and the rotor voltage vector as input, so the matrices in (18)–(23) can be computed using (16) and (17). The active and reactive power are estimated with the stator voltages and currents.

The control law is obtained by the minimization of the following cost function [29]:

$$J = (Y - w)^T W_y (Y - w) + U^T W_u U \tag{24}$$

where $w \in R^{(n_y\times q)\times 1}$ is the vector of the future output references to be controlled, $W_y \in R^{(n_y\times q)\times(n_y\times q)}$, $W_u \in R^{n_u\times n_u}$, $U \in R^{n_u\times n_u}$ is the input, q is the number of outputs, and n_u is the control horizon.

In the cost function presented in (24), the model is linearized and one can determine the minimal value algebraically. Since P_{px}, H, and D depend on estimated states, they must be updated for each control cycle. Substituting Y from (18) into (24) results in a quadratic cost function, dependent on U, which gives the analytical optimal solution

$$U = (H^TW_yH + W_u)^{-1}H^TW_y(w - P_{px}x(k) - D\omega_d(k)). \tag{25}$$

The diagram of the MBPC applied to DPC is shown in Fig. 2. The MBPC algorithm generates the rotor voltages that allows the active and reactive power convergence to their respective

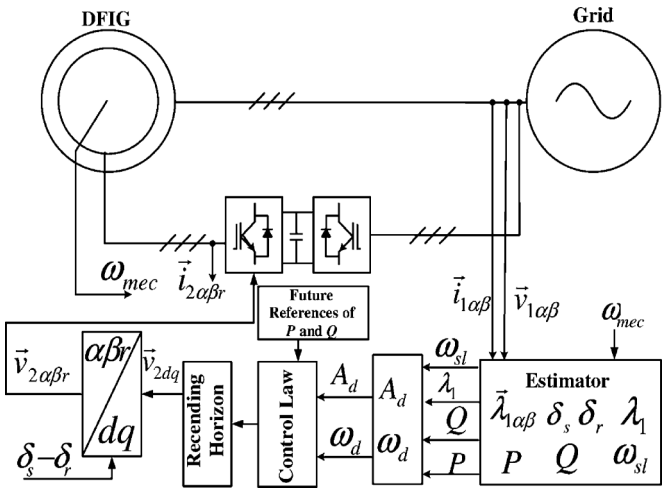

Fig. 2. Block diagram of proposed MBPC DPC strategy.

commanded values. The desired rotor voltage in the rotor $\alpha\beta r$ reference frame generates switching signals for the rotor side using either space vector modulation and it is given by $\vec{v}_{2\alpha\beta r} = \vec{v}_{2dq} e^{\delta_s - \delta_r}$.

In case of unbalanced grid supply, the DFIG has to be modeled considering these effects and one possibility can be seen in [40].

A. Estimation

Digital power control is required to calculate the active and reactive power values, their errors, the stator flux magnitude and position, the slip speed, and synchronous frequency.

The flux estimation using (1) is given by

$$\vec{\lambda}_{1\alpha\beta} = \int (\vec{v}_{1\alpha\beta} - R_1 \vec{i}_{1\alpha\beta}) dt \tag{26}$$

and the flux position by using (26) as

$$\delta_s = \arctan\left(\frac{\lambda_{1\beta}}{\lambda_{1\alpha}}\right). \tag{27}$$

Equation (26) can be implemented by using a low-pass filter [33]. The synchronous speed ω_1 estimation is given by

$$\omega_1 = \frac{d\delta_s}{dt} = \frac{(v_{1\beta} - R_1 i_{1\beta})\lambda_{1\alpha} - (v_{1\alpha} - R_1 i_{1\alpha})\lambda_{1\beta}}{(\lambda_{1\alpha})^2 + (\lambda_{1\beta})^2} \tag{28}$$

and the slip speed estimation by using the rotor speed and synchronous speed is

$$\omega_{\rm sl} = \omega_1 - PP\omega_{\rm mec}. \tag{29}$$

The angle between stator and rotor fluxes is given by

$$\delta_s - \delta_r = \int \omega_{\rm sl} dt. \tag{30}$$

Equation (30) can be implemented by using Euler's integer methods.

IV. Impact of Parameter Variations on System Performance

When the MBPC algorithm calculates the rotor voltages using (18)–(25), in the expressions of rotor voltage vector at any instant appears terms as shown in (31). The stator resistance used in stator flux estimation and the rotor resistance used in rotor voltage calculation have negligible impact on system performance for high power generators [19], [4]. The accuracy of the rotor voltage calculation is influenced by the constant σL_2 and the inductance ratio L_2/L_M that are determined by the stator and rotor leakage and mutual inductance. Since the leakage flux magnetic path is mainly air, the variation of the leakage inductance during operation is insignificant. However, mutual inductance variation needs to be considered due to possible variation of the magnetic permeability of the stator and rotor cores under different operating conditions. The required parameters can be simplified considering the relatively small leakage inductance L_{l1} and L_{l2} compared to the mutual inductance L_M that is shown in the Appendix, and it is given by

$$\frac{\sigma L_1 L_2}{L_M} \cong (L_{l1} + L_{l2}),\ \frac{L_2}{L_M} = \frac{L_M + L_{l2}}{L_M} \cong 1. \tag{31}$$

Equation (31) shows that the variations of L_M has little impact in $(\sigma L_1 L_2)/(L_M)$ and $(L_2)/(L_M)$. Therefore, its influence on the performance of the proposed control strategy would also be insignificant.

V. Simulation Results

The MATLAB/SimPowerSystems package was used in the simulation of the proposed control strategy. The power control strategy has the same time of the voltage source inverter sampling time and it is $T = 0.5 \times 10^{-4} s$. The DFIG parameters and values of n_u, n_y, W_y and W_u are shown in the Appendix. Fig. 2 shows the schematic of the implemented system and the inverter was modeled as controlled voltage sources, and the energy stored by the dc link capacitor was dissipated on a resistor load by using a hysteresis control of one IGBT in series with a diode.

To the power factor (PF) control, the reactive power reference is given by

$$Q_{\rm ref} = P_{\rm ref} \frac{\sqrt{1 - {\rm PF}^2}}{\rm PF}.$$

The DFIG was assumed to be in speed control, i.e., with the rotor speed set externally, since in a practical system, the wind turbine's large inertia results in slow rotor speed change [18], [19].

Initial studies with various active and reactive power steps and constant rotor speed at 226.6 rad/s were carried out to test the dynamic response of the proposed power control strategy, and it is shown in Fig. 3(a). The initial active power and power factor references were -60 kW and FP $= +0.85$. The active power and power factor references were step changed from -60 to -200 kW and from a PF of 0.85 to -0.85 at 2.5 s, and the power reference were step changed again from -100 to

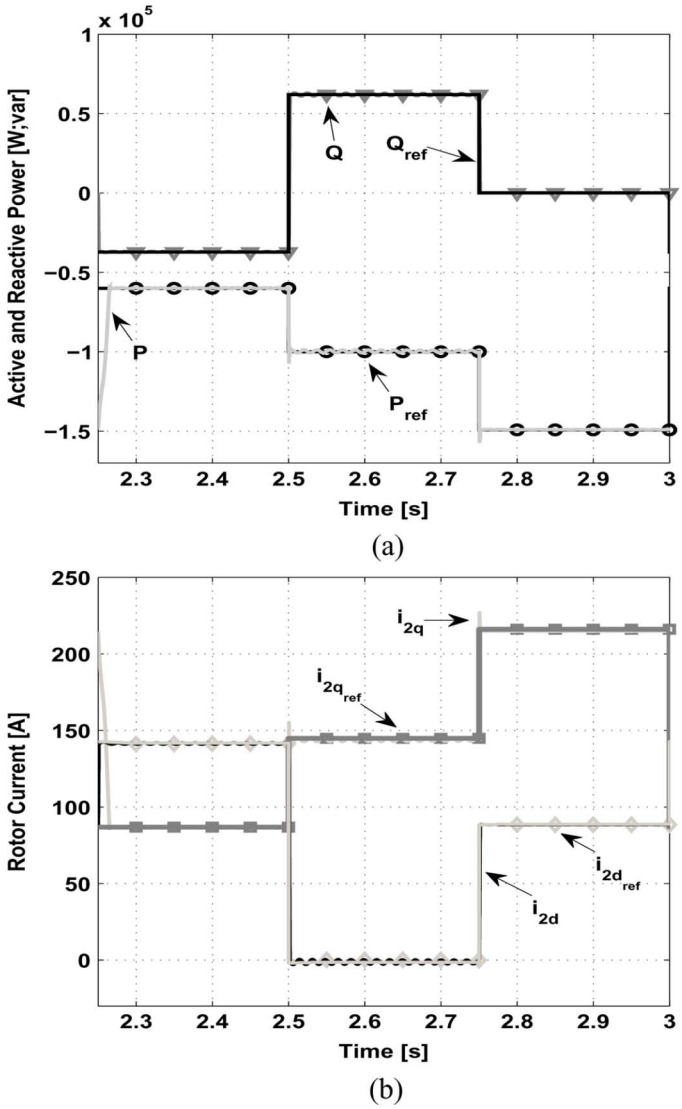

Fig. 3. Response of step tests for active and reactive power and rotor currents in supersynchronous operation. (a) Response of step of active and reactive power. (b) Response of step of rotor currents in synchronous referential.

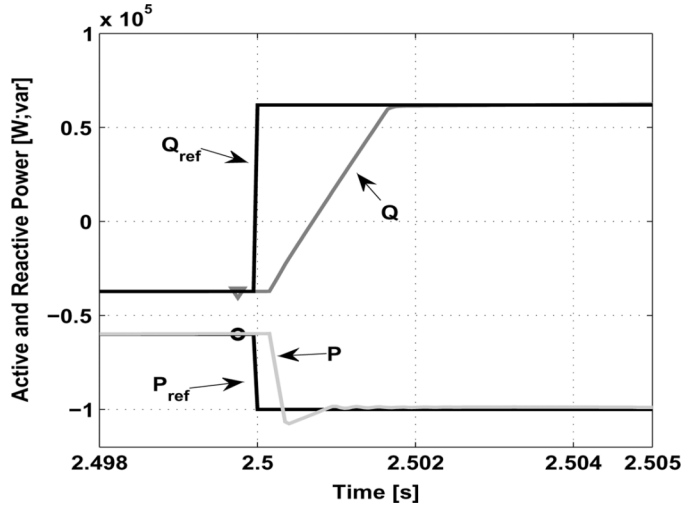

Fig. 4. Detailed active and reactive power responses.

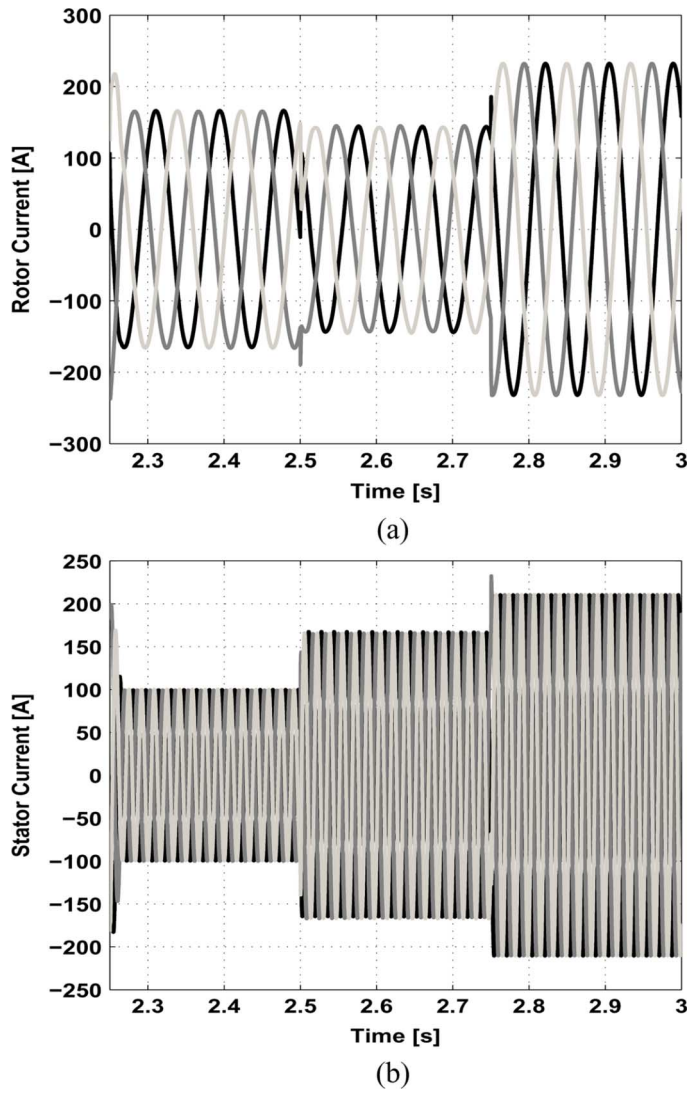

Fig. 5. Stator and rotor currents. (a) Rotor currents. (b) Stator currents.

−149.2 kW and from a PF of −0.85 to 1 at 2.75 s, respectively. The active and reactive power response in detail is shown in Fig. 4. The rotor currents in synchronous referential are shown in Fig. 3(b) and the rotor and stator currents in the stationary referential are shown in Fig. 5. It can be seen that the proposed MBPC strategy controls the rotor current vector in Fig. 3(b) although it does not have any rotor current loops in its formulation. The dynamic response of both active and reactive powers are in few milliseconds; there is no overshoot of either stator/rotor or the active/reactive powers and the satisfactory performance of the controller can be seen.

Studies with various power steps and rotor speed were carried out to further test the proposed power control strategy. During the period 1.65–2.1 s, the rotor speed increased from 151.1 to 226.6 rad/s. Fig. 6(a) shows the results step reference tests of active and reactive power. The power steps, i.e., active power and power factor references, were changed from −60 to −100 kW and from a PF of 0.85 to −0.85 at 2.5 s. The rotor currents in synchronous referential are shown in Fig. 6(b) and the rotor speed, the rotor and stator currents in the stationary referential are shown in Fig. 7. Again, it can be seen that the proposed

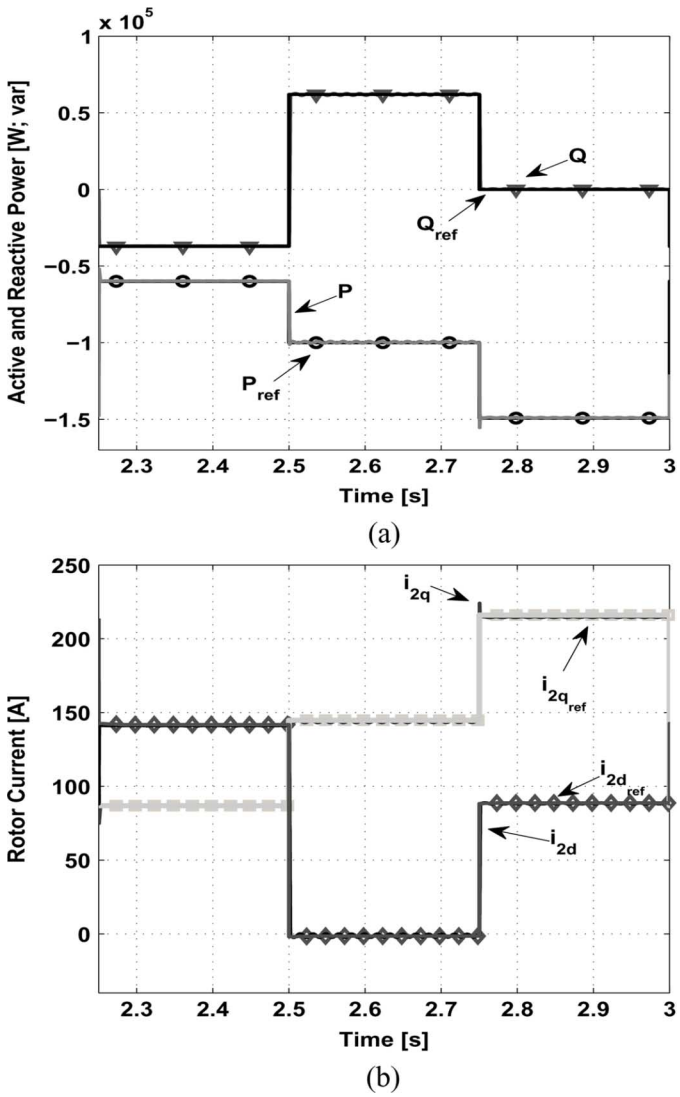

Fig. 6. Response of step tests for active and reactive power and rotor currents with several speed operations. (a) Response of step of active and reactive power. (b) Response of step of rotor currents in synchronous referential.

MBPC strategy controls the rotor current vector in Fig. 6(b) although it does not have any rotor current loops in its formulation. The controlled dc link voltage is shown in Fig. 8. The oscillations occur due to the fact that the voltage was controlled by a hysteresis controller. The satisfactory performance of the MBPC controller can be seen due to the fact that the active and reactive power reach their desired reference values when the rotor speed varies.

To test the impact of the parameter variations on the system performance, the rotor resistance R_2 and mutual inductance L_M are increased by 20%. The same tests of step reference of active and reactive powers with rotor speed variation and with parameter variation are shown in Figs. 9 and 10. Comparing Figs. 6 and 9 and Figs. 7 and 10, there is hardly any difference, and even with such large inductance and rotor resistance errors, the system maintains satisfactory performance under both steady-state and transient conditions.

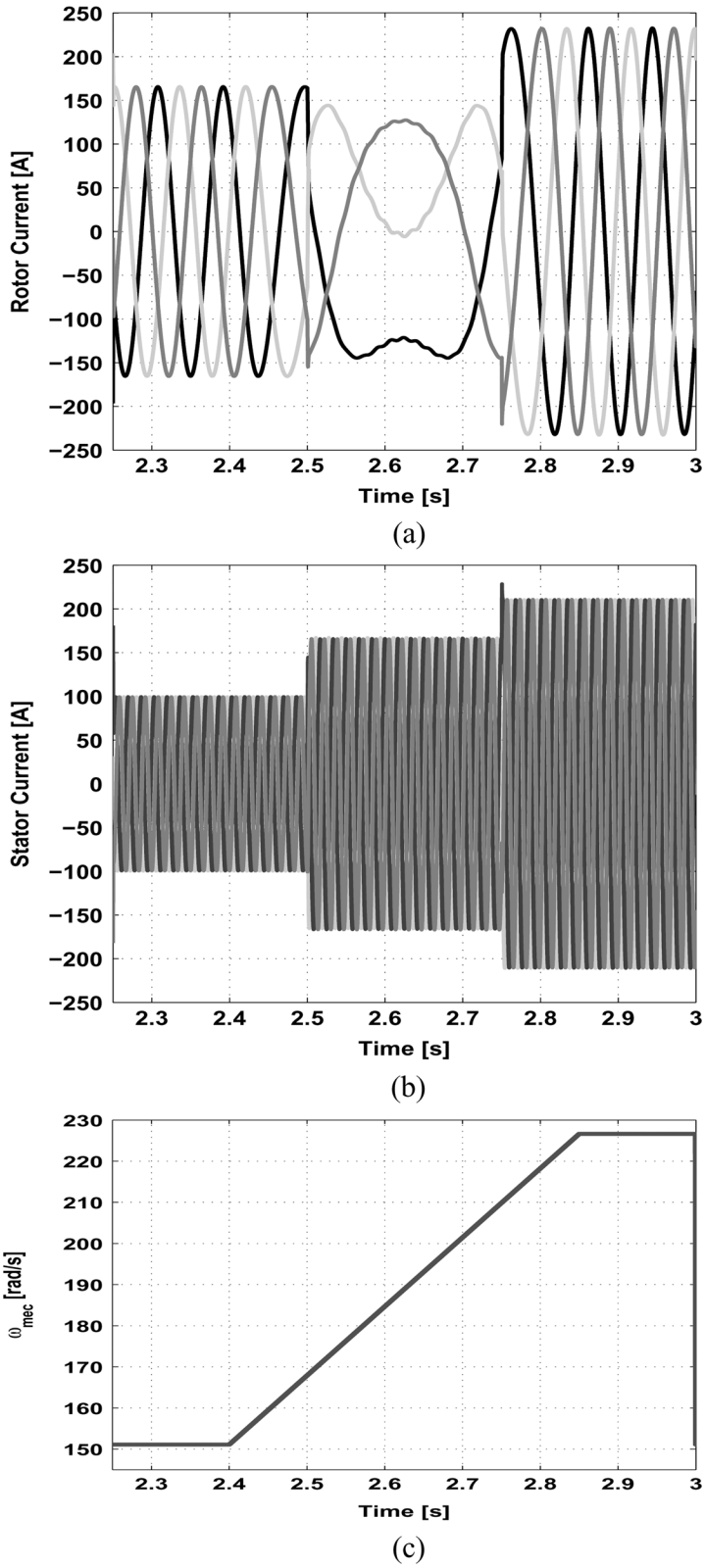

Fig. 7. Stator, rotor currents, and rotor speed. (a) Rotor currents. (b) Stator currents. (c) Rotor speed.

VI. Conclusion

This paper has presented a model-based predictive control applied to the DPC for DFIG. The control law is derived by

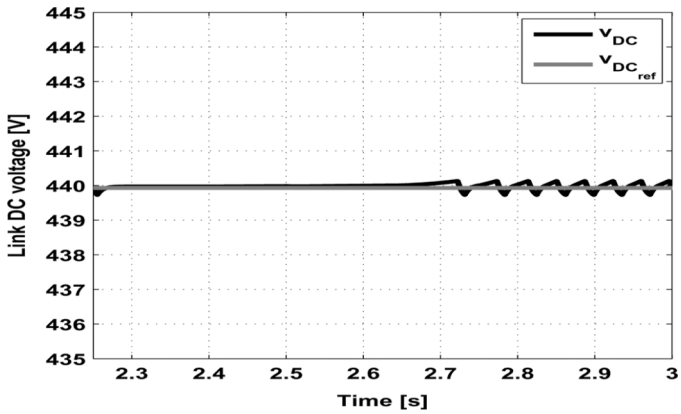

Fig. 8. DC link voltage.

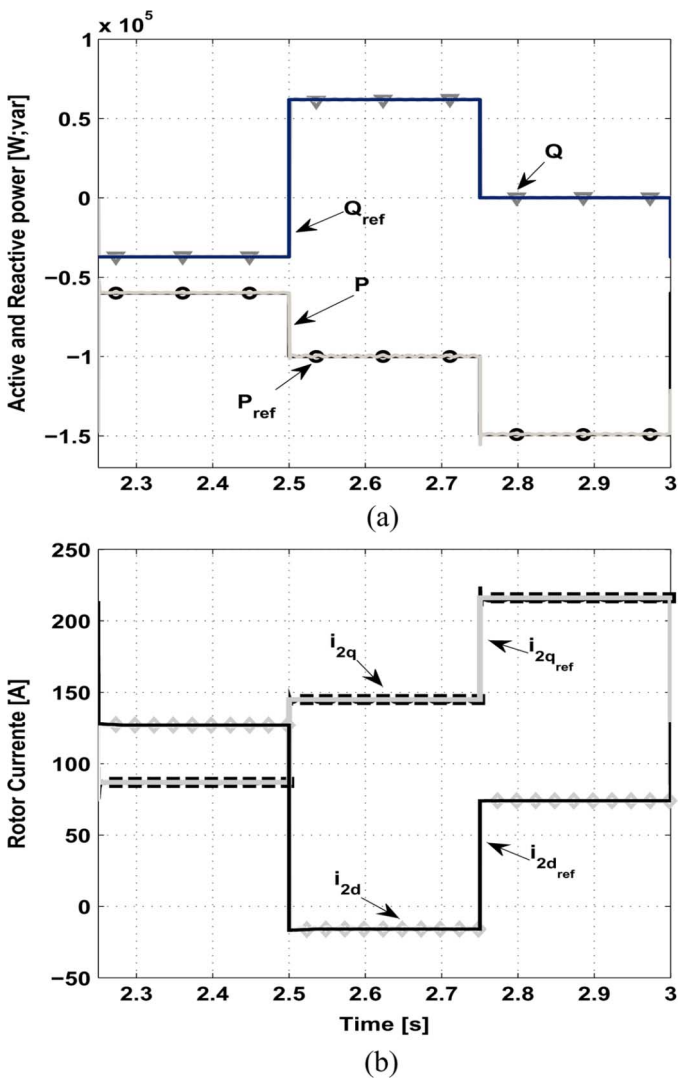

Fig. 9. Response of step tests for active and reactive power and rotor currents with several speed operations. (a) Response of step of active and reactive power. (b) Response of step of rotor currents in synchronous referential.

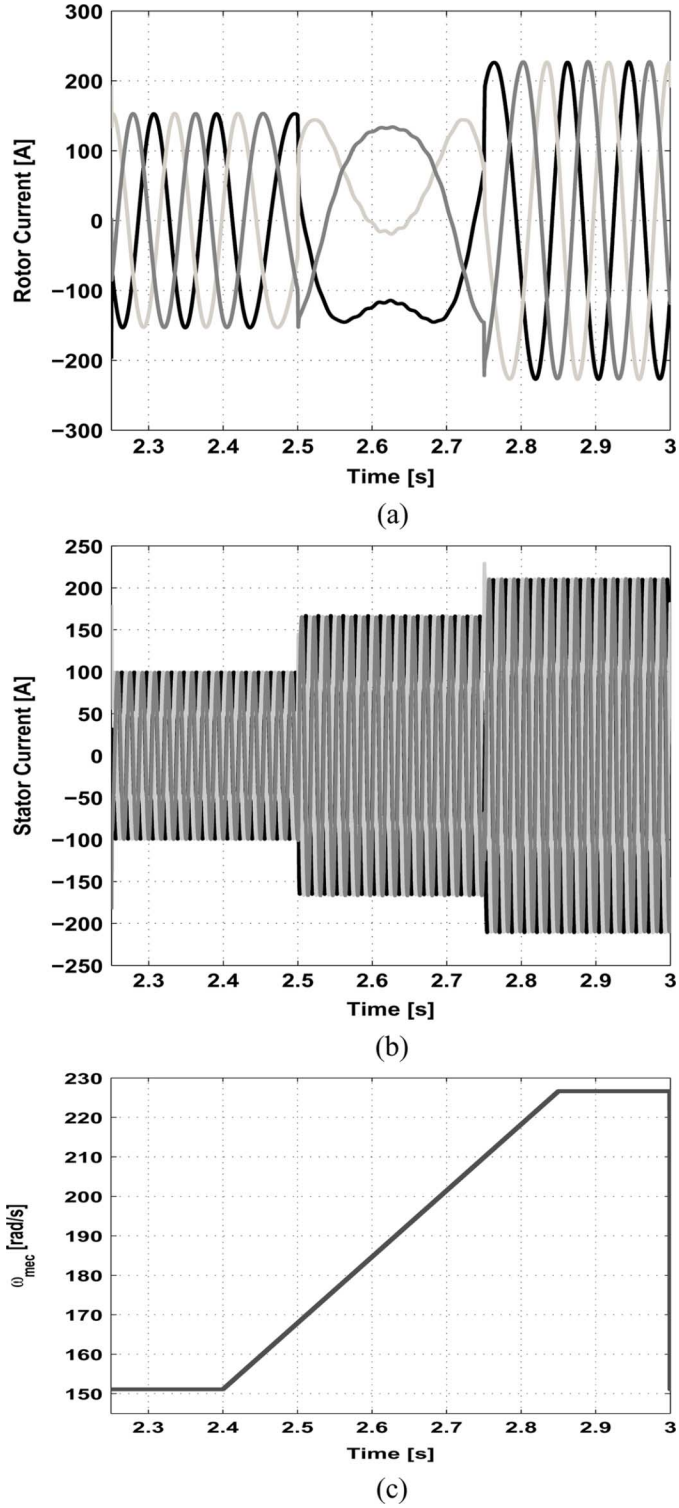

Fig. 10. Stator, rotor currents, and rotor speed. (a) Rotor currents. (b) Stator currents. (c) Rotor speed.

optimization of an objective function that considers the control effort and the difference between the predicted outputs (active and reactive power) and the specific references, with predicted outputs calculated using a linearized state-space model. This control law allows us to calculate the voltage to be applied on the rotor by using the system behavior for more than one single future sampling cycle. This strategy uses a constant switching frequency that overcomes the drawbacks of conventional DPC [17], [18] and does not use rotor current loops for the active and reactive power control.

The impact of machine parameters variations is analyzed and found to be negligible. The simulations confirm the effectiveness and the robustness of the predictive direct power controller during several operating conditions and variations of machine parameters.

Power generation is the focus in the wind energy systems. Thus, the DPC strategy does not need an out loop for power control as the rotor current control strategy and it becomes an alternative power control strategy for this purpose. Hence, this DPC strategy becomes an interesting tool for DFIG power control implementation.

APPENDIX

A. Effect of Parameters in the Rotor Voltage Calculation

Considering that $L_{l1} \ll L_M$ and $L_{l2} \ll L_M$, the $(\sigma L_1 L_2)/(L_M)$ and $(L_2)/(L_M)$ can be simplified as

$$\begin{aligned}\frac{\sigma L_1 L_2}{L_M} &= \frac{L_1 L_2 - L_M^2}{L_M} \\ &= \frac{(L_{l1}L_{l2}) + L_M(L_{l1} + L_{l2}) + L_M^2 - L_M^2}{L_M} \\ &\cong (L_{l1} + L_{l2})\end{aligned}$$

and

$$\frac{L_2}{L_M} = \frac{L_M + L_{l2}}{L_M} = 1 + \frac{L_{l2}}{L_M}.$$

B. DFIG Parameters

$R_1 = 0.02475\ \Omega$; $R_2 = 0.0133\ \Omega$; $L_m = 0.01425$ H; $L_{l1} = 0.000284$ H; $L_{l2} = 0.000284$ H; $J = 2.6\ \text{Kg}\cdot\text{m}^2$; $PP = 2$; $PN = 149.2$ kVA; $V_N = 575$ V; $n_u = 1$; $n_y = 2$

$$W_y = \begin{bmatrix} 10 & 0 \\ 0 & 1 \end{bmatrix} \quad \text{and} \quad W_u = \begin{bmatrix} 25 & 0 \\ 0 & 15 \end{bmatrix}.$$

REFERENCES

[1] G. Abad, J. López, M. A. Rodríguez, L. Marroyo, and G. Iwanski, *Doubly Fed Induction Machine Modeling and Control for Wind Energy Generation*. Hoboken, NJ: Wiley, 2011.

[2] R. Datta and V. T. Rangathan, "Variable-speed wind power generation using doubly fed wound rotor induction machine—A comparison with alternative schemes," *IEEE Trans. Energy Convers.*, vol. 17, no. 3, pp. 414–421, Sep. 2002.

[3] B. H. Chowdhury and S. Chellapilla, "Double-fed induction generation control for variable speed wind power generation," *Elect. Power Syst. Res.*, no. 76, pp. 786–800, 2006.

[4] B. Hopfensperger, D. J. Atkinson, and R. Lakin, "Stator-f lux-oriented control of a doubly-fed induction machine with and without position encoder," in *Proc. Inst. Elect. Eng., Elect. Power Applications*, Apr. 2000, vol. 147, no. 4, pp. 241–250.

[5] A. Tapia, G. Tapia, J. X. Ostolaza, and J. R. Sáenz, "Modeling and control of a wind turbine driven doubly fed induction generator," *IEEE Trans. Energy Convers.*, vol. 18, no. 2, pp. 194–204, Jun. 2003.

[6] J. P. da Costa, J. Marques, H. A. Gründling, and H. Pinheiro, "Dynamic behavior of the doubly-fed induction generator in stator flux vector reference frame," *Eletrônica de Potência*, vol. 13, no. 1, pp. 33–42, Mar. 2006.

[7] R. G. de Oliveira, J. L. da Silva, and S. R. Silva, "Development of a new reactive power control strategy in doubly-fed induction generators for wind turbines," *Eletrônica de Potência*, vol. 13, no. 4, pp. 277–284, Nov. 2008.

[8] F. P., T. Bouaouiche, and M. Machmoum, "Advanced control of a doubly-fed induction generator for wind energy conversion," *Elect. Power Syst. Res.*, vol. 79, pp. 1085–1096, 2009.

[9] Z. Xin-fang, X. Da-ping, and L. Yi-bing, "Predictive functional control of a doubly fed induction generator for variable speed wind turbines," in *Proc. IEEE World Congress on Intelligent Control and Automation*, Hangzhou, China, Jun. 15–19, 2004, pp. 3315–3319.

[10] J. Morren and S. W. H. de Haan, "Ridethrough of wind turbines with doubly-fed induction generator during a voltage dip," *IEEE Trans. Energy Convers.*, vol. 20, no. 2, pp. 435–441, Jun. 2005.

[11] J. Guo, X. Cai, and Y. Gong, "Decoupled control of active and reactive power for a grid-connected doubly-fed induction generator," in *Proc. Third Int. Conf. Electric Utility Deregulation and Restructuring and Power Technologies (DRPT)*, Apr. 2008, pp. 2620–2625.

[12] J. P. A. Vieira, M. V. A. Nunes, U. H. Bezerra, and A. C. do Nascimento, "Controladores fuzzy aplicados ao conversor de geradores de indução duplamente excitados em sistemas eólicos integrados a sistemas de potência," *Revista Controle & Automação*, vol. 18, no. 1, pp. 115–126, Jan./Feb./Mar. 2007.

[13] X. Yao, Y. Jing, and Z. Xing, "Direct torque control of a doubly-fed wind generator based on grey-fuzzy logic," in *Proc. Int. Conf. Mechatronics and Automation (ICMA 2007)*, Aug. 2007, pp. 3587–3592.

[14] I. Takahashi and T. Noguchi, "A new quick-response and high-efficiency control strategy of an induction motor," *IEEE Trans. Ind. Appl.*, vol. IA-22, no. 5, pp. 820–827, Sep./Oct. 1986.

[15] M. Depenbrock, "Direct self-control(dsc) of inverter-fed induction machine," *IEEE Trans. Power Electron.*, vol. 3, no. 4, pp. 420–429, Oct. 1988.

[16] T. Noguchi, H. Tomiki, S. Kondo, and I. Takahashi, "Direct power control of pwm converter without power-source voltage sensors," *IEEE Trans. Ind. Appl.*, vol. 34, no. 3, pp. 473–479, May/Jun. 1998.

[17] R. Datta and V. T. Ranganathan, "Direct power control of grid-connected wound rotor induction machine without rotor position sensors," *IEEE Trans. Power Electron.*, vol. 16, no. 3, pp. 390–399, May 2001.

[18] L. Xu and P. Cartwright, "Direct active and reactive power control of dfig for wind energy generation," *IEEE Trans. Energy Convers.*, vol. 21, no. 3, pp. 750–758, Sep. 2006.

[19] D. Zhi and L. Xu, "Direct power control of dfig with constant switching frequency and improved transient performance," *IEEE Trans. Energy Convers.*, vol. 22, no. 1, pp. 110–118, Mar. 2007.

[20] G. Xiao-Ming, S. Dan, H. Ben-Teng, and H. Ling-Ling, "Direct power control for wind-turbine driven doubly-fed induction generator with constant switch frequency," in *Proc. Int. Conf. Electrical Machines and Systems*, Oct. 2007, pp. 253–258.

[21] D. Santos-Martin, J. L. Rodriguez-Amenedo, and S. Arnalte, "Direct power control applied to doubly fed induction generator under unbalanced grid voltage conditions," *IEEE Trans. Power Electron.*, vol. 13, no. 5, pp. 115–126, Sep. 2008.

[22] D. Sun, X. Guo, L. Shang, and Y. He, "Modified dpc for dfig based wind power generation under unbalanced grid-voltage," in *Proc. Int. Conf. Electrical Machines and Systems (ICEMS 2008)*, Oct. 2008, pp. 2299–2304.

[23] R. Kennel, A. Linder, and M. Linke, "Generalized predictive control (gpc)-ready for use in driveapplications?," in *Proc. IEEE Power Electronics Specialists Conf. (PESC)*, 2001, vol. 4, pp. 1839–1844.

[24] H. Abu-Rub, J. Guzinski, Z. Krzeminski, and H. A. Toliyat, "Predictive current control of voltage-source inverters," *IEEE Trans. Ind. Electron.*, vol. 51, no. 3, pp. 585–593, Jun. 2004.

[25] L. Zhang, R. Norman, and W. Shepherd, "Long-range predictive control of current regulated pwm forinduction motor drives using the synchronous reference frame," *IEEE Trans. Control Syst. Technol.*, vol. 5, no. 1, pp. 119–126, Jan. 1996.

[26] E. S. de Santana, E. Bim, and W. C. do Amaral, "A predictive algorithm for controlling speed and rotor flux of induction motor," *IEEE Trans. Ind. Electron.*, vol. 55, no. 12, pp. 4398–4407, Dec. 2008.

[27] L. Xu, D. Zhi, and B. W. Williams, "Predictive current control of doubly fed induction generators," *IEEE Trans. Ind. Electron.*, vol. 56, no. 10, pp. 4143–4153, Oct. 2009.

[28] G. Abad, M. Rodríguez, and J. Poza, "Three-level npc converter-based predictive direct power control of the doubly fed induction machine at low constant switching frequency," *IEEE Trans. Ind. Electron.*, vol. 55, no. 12, pp. 4417–4429, Dec. 2008.

[29] A. J. S. Filho, M. E. de Oliveira Filho, and E. Ruppert, "A predictive power control for wind energy," *IEEE Trans. Sustain. Energy*, vol. 2, no. 1, pp. 97–105, Jan. 2011.

[30] W. Leonhard, *Control of Electrical Drives*. Berlin, Heidelberg, New York, Tokyo: Springer-Verlag, 1985.
[31] S. Yamamura, *Spiral Vector Theory of AC Circuits and Machines*. Oxford: Clarendon Press, 1992.
[32] J. Holtz, J. Quan, J. Pontt, J. Rodríguez, P. Newman, and H. Miranda, "Design of fast and robust current regulators for high-power drives based on complex state variables," *IEEE Trans. Ind. Appl.*, vol. 40, no. 5, pp. 1388–1397, Sep./Oct. 2004.
[33] A. J. S. Filho and E. R. Filho, "The complex controller for three-phase induction motor direct torque control," *Sba Controle e automação.*, vol. 20, no. 2, pp. 256–262, 2009.
[34] G. F. Franklin, J. D. Powel, and M. L. Workman, *Digital Control of Dynamic Systems*. Reading, MA: Addison-Wesley, 1994.
[35] A. Linder and R. Kennel, "Direct model predictive control—A new direct predictive control strategy for electrical drives," in *Proc. Eur. Conf. Power Electronics and Applications*, Dresden, Germany, Sep. 11–14, 2005, 10 pp..
[36] A. J. S. Filho, M. de Oliveira Filho, and E. R. Filho, "A digital active and reactive power control for doubly-fed induction generetator," in *Proc. IEEE Power Electronics Specialists Conf. (PESC)*, Jun. 2008, pp. 2718–2722.
[37] J. A. Rossiter, *Model Based Predictive Control—A Practical Approach*. Boca Raton, FL: CRC Press, 2003.
[38] P. Cortes, M. Kazmierkowski, R. Kennel, D. Quevedo, and J. Rodriguez, "Predictive control in power electronics and drives," *IEEE Trans. Ind. Electron.*, vol. 55, no. 12, pp. 4312–4324, Dec. 2008.
[39] H. Miranda, P. Cortes, J. Yuz, and J. Rodriguez, "Predictive torque control of induction machines based on state-space models," *IEEE Trans. Ind. Electron.*, vol. 56, no. 6, pp. 1916–1924, Jun. 2009.
[40] H. Nian, Y. Song, P. Zhou, and Y. He, "Improved direct power control of a wind turbine driven doubly fed induction generator during transient grid voltage unbalance," *IEEE Trans. Energy Convers.*, vol. 26, no. 3, pp. 976–986, Sep. 2011.

Alfeu J. Sguarezi Filho (S'03–A'05–M'11) received the bachelor degree in electrical engineering from Faculdade Área 1, in 2005, and the Master and Ph.D. degrees from Campinas University, Campinas, Brazil, in 2007 and 2010, respectively.

He was working as researcher at Campinas University under the FAPESP postdoctoral program from 2010 to 2011. He is a professor at Universidade Federal do ABC—UFABC, in Santo André, Brazil, teaching in the areas of electrical machines, power electronics, and electrical drives. His research interests are machine drives, doubly-fed induction generators, power control, and electrical power systems.

Ernesto Ruppert Filho received the bachelor degree in electrical engineering and the Master and Ph.D. degrees from Campinas University, Campinas, Brazil, in 1971, 1974, and 1983, respectively.

From 1972 to 1978, he had been working at the Electrical and Computer Engineering School, Campinas University, as an Assistant Professor in the Electromechanical Energy Conversion area. From 1979 to 1983, he worked for General Electric in Brazil designing large induction and synchronous motors and worked as an Application Engineer dedicated to large motors and generators. From 1983 to 1989, he worked for Vigesa Heavy Equipments in Brazil designing very large hydrogenerators and also performing commissioning tests in some hydro power plants in Brazil. From 1989 to 1992, he ran his own company dealing with electrical installations. Since 1992, he has been working as a Full Professor at the Electrical and Computer Engineering School of Campinas University, researching and teaching in the areas of electrical machines, power electronics, drives, and electrical power systems.